JOURNAL OF CATALYSIS 137, 437–452 (1992)

Kinetics of Cracking of *n*-Decane and *n*-Hexane on Zeolites H-ZSM-5 and HY in the Temperature Range 500 to 780 K

LOTHAR RIEKERT[1] AND JIAN-QING ZHOU

Institut für Chemische Verfahrenstechnik der Universität Karlsruhe, D-7500 Karlsruhe, Germany

Received December 16, 1991; revised May 22, 1992

The kinetics of cracking of *n*-decane and *n*-hexane were investigated by observing the composition of the gas phase in contact with zeolite catalysts H-ZSM-5 and HY in a well-mixed closed system (gradientless batch-reactor). Catalyst temperature was varied from 200°C (473 K) to 500°C (773 K); partial pressure of reactant paraffin between 0.5 and 20 mbar. For ZSM-5 the influence of crystal size and of Si/Al-ratio on the kinetics was investigated. At temperatures above 400°C (673 K), the rates of cracking on H-ZSM-5 are first order in the partial pressures of paraffin; an estimate of diffusivity under reaction conditions is obtained from the influence of crystal size on observed rates at $T > 700$ K. Between 200°C (473 K) and 400°C (673 K), the rate of reaction of pure *n*-decane on H-ZSM-5 exhibits a maximum near 300°C and decreases with temperature to a minimum near 360°C. An induction period followed by autocatalysis was observed with *n*-decane as reactant in this temperature-range, depending on Si/Al ratio and degree of deactivation of the zeolite. It can be suppressed by addition of olefin to reactant paraffin. These phenomena are also observed in a less pronounced way with dealuminated HY, which deactivates more rapidly. A mathematical model based on a dual pathway of carbenium ion and protolytic cracking as postulated by Haag and Dessau (*in* "Proceedings 8th International Congress on Catalysis, Berlin 1984," Vol. II, p. 305, Verlag Chemie, Weinheim, 1984) represents the observations qualitatively and in an approximate way also quantitatively. © 1992 Academic Press, Inc.

INTRODUCTION

The subject of this paper is the kinetics of the cracking of alkanes (paraffins) in zeolite catalysts, mainly ZSM-5. The abundant literature on this commercially important subject has been reviewed by Jacobs (*1*), Venuto and Habib (*2*), and by Wojciechowski and Corma (*3*). This literature concerns mainly the merits of zeolites as a component in commercial cracking catalysts on the one hand, whereas on the other hand the mechanism of the reaction has been debated rather extensively, based on observations obtained with integral reactors. Detailed quantitative kinetic data are rather scarce. To obtain them from observation of integral conversion at different operating conditions is cumbersome and difficult if the properties of the catalyst depend upon time-on-stream. We have therefore adopted a novel experimental procedure in order to observe the kinetics in more detail, which consists in monitoring the gas phase composition in a well-mixed closed system (gradientless batch-reactor) as a function of contact time between catalyst and hydrocarbons. Time-on-stream and run time are here identical when starting with a fresh or regenerated catalyst; rate and product composition can be obtained for a wide range of conversion in a single experiment for a given catalyst, temperature, and initial composition. This experimental procedure mimics the conditions in a commercial riser-reactor, where catalyst and reacting hydrocarbons travel together through the reaction zone. However, the experimental results described below were obtained at partial pressures

[1] To whom correspondence should be addressed.

0021-9517/92 $5.00
Copyright © 1992 by Academic Press, Inc.
All rights of reproduction in any form reserved.

of hydrocarbons in the mbar range, so extrapolation to the operating range of a commercial unit should be done with caution.

The main body of the investigation concerns the reaction of *n*-decane on zeolite H-ZSM-5; in addition we studied the influence of paraffin chain length (n-C_6H_{14} vs n-$C_{10}H_{22}$) and of zeolite structure (HY vs H-ZSM-5) on some of the observed phenomena.

EXPERIMENTAL

1. Zeolites

Zeolites ZSM-5 were synthesized by crystallization without agitation within 4 days under autogenous pressure. Gel-composition corresponded to

$$36\ \mathrm{PA} \cdot \mathrm{Al_2(SO_4)_3} \cdot l\ \mathrm{SiO_2} \cdot m\ \mathrm{NaOH} \cdot n\ \mathrm{H_2O}$$

with $l = 88 - 320$, m = 7 – 28, n = 1000 – 4000 (PA = $C_3H_7NH_2$); Different crystal sizes were obtained by variation of crystallization temperature (433 to 458 K) and of pH. The resulting crystalline materials were shown by XRD to correspond to the MFI-structure with 100% crystallinity. The zeolites were calcined in air at 823 K for 20 h, then exchanged three times with excess 1 *M* NH_4Cl solution at 373 K for 4 h, and washed and dried at 393 K. Through subsequent calcination at 823 K in air for 20 h the ammonium form was converted to the hydrogen form (H-ZSM-5).

Zeolite HY with an Si/Al-ratio of 11 was prepared by dealumination of NaY (Baylith C-P 116 with Si/Al = 2.5 from Bayer AG, Leverkusen) through reaction with $SiCl_4$ at 673 K, and subsequent treatment with 0.1 *M* HCl at 363 K, as described by Beyer *et al.* (*4*a). Si/Al = 11 was determined by chemical analysis, whereas Si/Al = 12 was found from the lattice constant (a_o = 2.44 nm), according to Breck and Flanigan (*4*b). The Na-content was below 0.2 wt%.

Crystal sizes were determined by scanning electron microscopy (SEM); the variance within each sample was less than 10%. The characteristic length l is defined as the ratio of volume to (external) surface of the crystals. Zeolites used as catalysts are listed in Table 1; the designations of zeolites ZSM-5 used in the following indicate composition and crystal size. The zeolites were pressed (1900 bar) into pellets without any binder, the pellets were crushed, and a particle-size fraction of 0.5–1 mm to be used as catalysts was obtained by sieving.

2. Observation of Kinetics

The batch reactor used for kinetic measurements is shown schematically in Fig. 1; the apparatus has been described previously (*5*). Before an experiment the mixing turbine and the quartz-reactor are disconnected, the zeolite in the reactor (between 0.05 and 0.3 g) is heated to 823 K in an air-stream for 2 h, then brought to reaction temperature under nitrogen. The mixing turbine (V = 7100 cm^3) is kept at 453 K as are all connecting lines and valves; it is filled with nitrogen at atmospheric pressure and the reactant hydrocarbon is added by injection through a septum. The mixing turbine and the reactor loop are connected at $t = 0$ to start a run, a gas stream of 200 $cm^3\ s^{-1}$ is then passed from the mixing turbine through the catalyst bed and back to the mixer by means of a membrane pump operating also at 453 K. The reactor itself operates in the differential mode and the gas phase in the closed system consisting of mixing turbine and reactor-loop can be considered as well-mixed; its composition is determined periodically by GC (capillary column of 0.2 mm diameter and 50 m length, methyl silicone gum as stationary phase) with an FID detector. The blind activity of the system was negligible at temperatures of the reactor up to 850 K; all observed reaction rates were proportional to the mass of zeolite catalyst in the system. Besides clock time t, a modified time coordinate τ can therefore be used, defined as

$$\tau \equiv t \cdot m,$$

TABLE 1

Zeolites

Structure	Si/Al	Size (μm)	l (μm)	Designation
MFI (H-ZSM-5)	22	15 × 4 × 4	0.9	22/9
	44	2.6 dia.	0.4	44/4
	44	9 × 3 × 3	0.6	44/9
	44	14 × 4 × 4	0.9	44/9
	44	17 × 10 × 10	1.9	44/19
	44	36 × 10 × 10	2.2	44/22
	100	16 × 4 × 4	0.9	100/9
	160	3.0 dia.	0.5	160/5
FAU (HY)	11			Y11

where m is the mass of zeolite in the reactor and τ is equivalent to modified space time in a fixed bed with plug flow; conversion and product composition depend only on τ for a given zeolite, temperature, and initial composition.

Gas-phase composition is described by carbon fractions y_i, defined as amount of carbon in gaseous compound i divided by the amount of carbon initially introduced as reactant A

$$y_i \equiv \frac{n_c \text{ in } i}{n_c \text{ in A at } t = 0}.$$

We have

$$\text{at } t = 0: \quad y_A = 1;$$
$$\text{at } t > 0: \quad X = 1 - y_A,$$

with $X \equiv$ conversion of reactant A. The rate of the reaction

$$(A)_{gas} \rightarrow \text{cracked products}$$

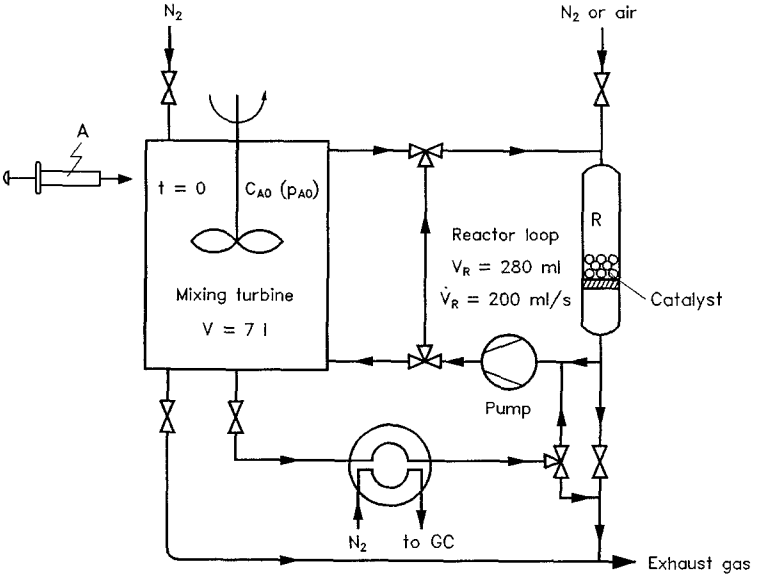

FIG. 1. Batch-reactor system (schematic).

in mol g^{-1} s^{-1} can be obtained from the graphs of X vs τ as

$$r_m = \frac{1}{m} \cdot \left(-\frac{dn_A}{dt}\right) = 1.91 \times 10^{-4}\,\text{mol} \cdot \frac{p_{A_0}}{\text{mbar}} \cdot \frac{dX}{d\tau}, \quad (1)$$

where p_{A_0} represents the initial partial pressure of reactant A at t = 0. The integral selectivity S_i of conversion of reactant A to hydrocarbon i is

$$S_i = \frac{y_i}{1 - y_A} = \frac{y_i}{X}. \quad (2)$$

Reactants *n*-decane and *n*-hexane were both standard for GC, obtained from Fluka Chemie AG and used without further purification.

The observed rates of reaction were not influenced by mass-transfer to the pellets or by intercrystalline diffusion in the voids within the pellet. Even for the highest rate of reaction observed (*n*-decane on zeolite 44/4 at 773 K) for pellets of 1 mm diameter, a Weisz number $\Phi \tanh \Phi \approx 0.08$ was evaluated assuming $D_{\text{eff}} = 0.1$ cm^2 s^{-1} for the intercrystalline diffusion.

RESULTS

1. n-Decane/H-ZSM-5

Conversion X versus time τ observed with fresh zeolite 44/4 is shown in Fig. 2a for three temperatures. The initial rate of reaction decreases with increasing temperature; at 648 K the S-shaped-curve of X vs τ indicates autocatalytic behavior. Figure 2b shows the temperature-dependence of the initial rate of reaction observed for constant initial concentration of decane at low conversion ($X = 0.05$). It is "N-shaped," reaching a maximum around 560 K, then decreasing to a minimum around 630 K, whereafter it increases monotonically. We shall first consider the kinetics at high temperatures ($T > 673$ K) and then in the range below 650 K.

(a) Kinetics at $T \geq 673$ K. For initial partial pressures of *n*-decane between 0.5 and 20 mbar, H-ZSM-5 did not deactivate at $T \geq 673$ K. Kinetics were found to be reproducible in successive runs without treating the catalyst between runs with air at 823 K. This result was corroborated by observation of the reaction in an integral reactor at 723 K, $p_{A_0} = 2.5$ mbar in N_2, where conversion remained constant ($X = 0.45$) for more than 1 h. The conversion

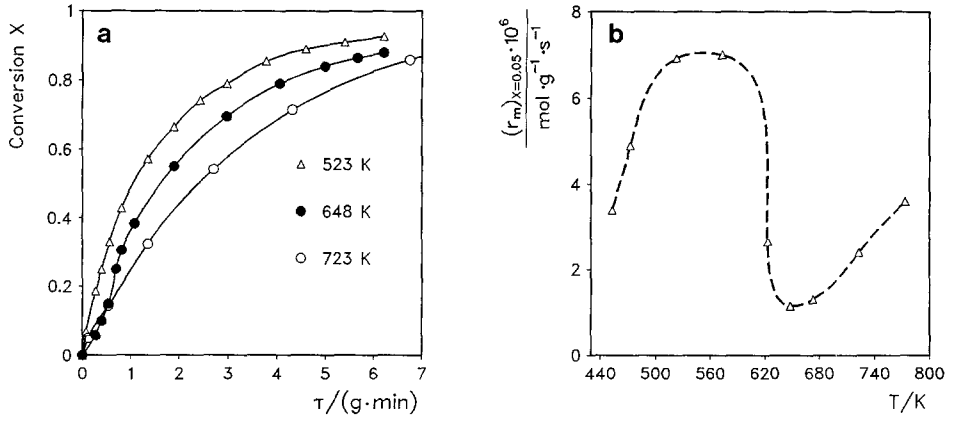

FIG. 2. Influence of temperature on rate of reaction of *n*-decane on zeolite 44/4, $p_{A_0} = 2.5$ mbar. (a) conversion X vs τ for three temperatures; (b) mass-specific rate of reaction at $X = 0.05$ as function of temperature.

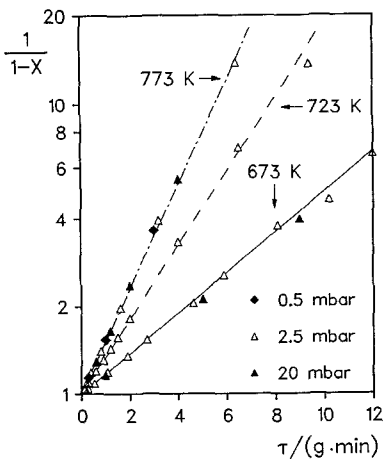

FIG. 3. First-order plot of conversion vs $\tau = t \cdot m$ on zeolite 44/4 for different initial partial pressures of reactant *n*-decane; $m = 0.08$ to 0.27 g.

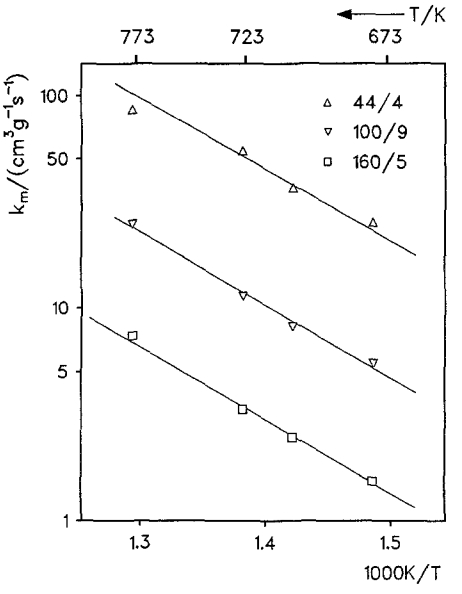

FIG. 4. Dependence of mass-specific rate coefficient k_m on temperature for cracking of *n*-decane on zeolites H-ZSM-5 at $T \geq 673$ K.

of *n*-decane is first order in the concentration of reactant as shown in Fig. 3, where $1/(1 - X)$ is plotted logarithmically against time τ, resulting in straight lines through the origin which are independent of p_{A_0} in the range 0.5 to 20 mbar. The temperature dependence of mass specific first order rate constants k_m for the reaction

$$(C_{10}H_{22})_g \rightarrow \text{products}$$

is shown in Fig. 4 for three zeolites with different Si/Al ratios.

The temperature coefficient corresponds to an activation energy of 62 kJ/mol, independent of Si/Al ratio, whereas the frequency factor was found to be approximately proportional to the square of the Al content. Data points shown in Fig. 4 refer to relatively small crystals of the most active zeolite with Si/Al = 44. For larger crystals the rate depends also on crystal size as shown in Fig. 5 for zeolites of constant composition (Si/Al = 44) but different size. At 723 K (450°C) the rate decreases when crystal size increases if the characteristic length l exceeds 1 μm; at 773 K this influence is already apparent for $l > 0.5$ μm.

(b) Kinetics at $T < 650$ K. At temperatures below 650 K zeolite ZSM-5 deactivates to a limited extent in contact with reactant and products. The zeolites can be fully regenerated by heating in a stream of air as described above; rates and product distributions on the regenerated catalysts were found to be identical to the respective observations on the fresh zeolites.

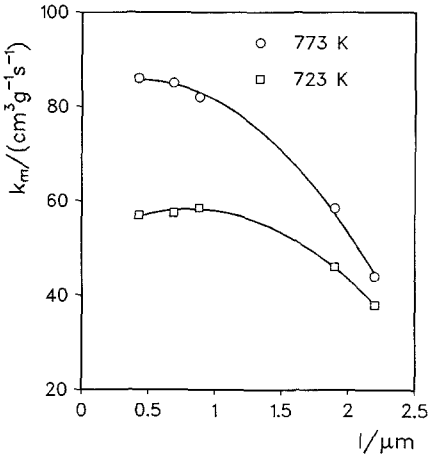

FIG. 5. Dependence of rate coefficient k_m of decane-cracking on crystal size for H-ZSM-5 with Si/Al = 44.

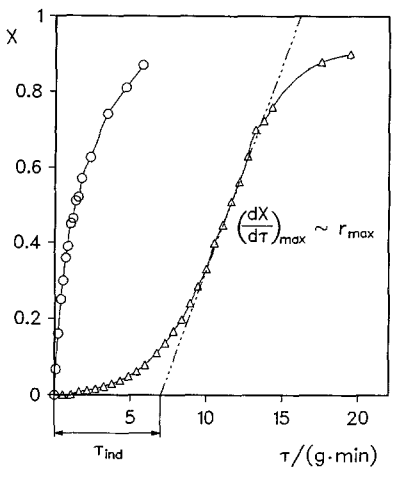

FIG. 6. X vs τ on zeolite 44/4 at 523 K; p_{A_0} = 2.5 mbar. (○) first run on fresh catalyst; (△) second run without preceding regeneration.

Deactivation does not cause simply a reduction of reaction rate but its effect is more complex, as shown in Fig. 6, where conversion at 523 K is plotted against τ for the first run on a fresh sample of zeolite 44/4 and for the second run without regeneration, the catalyst being kept under nitrogen between the first and second experiment. An induction period τ_{ind} is observed in the second run, which is operationally defined by the S-shaped curve of X vs τ as indicated in the figure. Thereafter the rate of reaction at a conversion around 60% almost equals the value observed in the first experiment for the not deactivated zeolite at the same degree of conversion.

Induction period and autocatalytic behavior, which results in an S-shaped curve of conversion vs time, were also reproducibly observed on fresh or regenerated catalysts, depending on zeolite composition (Si/Al ratio) and temperature. These observations can be quantified somewhat summarily by the length τ_{ind} of the induction period on the axis of modified time τ and the maximum rate of reaction $(r_m)_{max}$, observed at the point of inflection of X vs τ if the curve is S-shaped.

These data are listed in Table 2. The length of the induction period and the width of the temperature interval where it can be observed increase with Si/Al ratio in the zeolite. τ_{ind} vanishes generally at temperatures above 670 K and, depending on Si/Al ratio, also at low temperatures. The maximum rate r_m at a given temperature increases with the aluminium content in the zeolite; for a given zeolite $(r_m)_{max}$ decreases with increasing temperature, goes through a minimum and then rises in the high-temperature regime ($T \geq 673$ K) where no induction period was observed. The data in Table 2 refer to the first run with virgin or regenerated zeolites, except for zeolite 44/4 where observations in the first run at different temperatures are compared with those obtained in the second run at the same temperature without regeneration (cf. Fig. 6). The effect of deactivation is roughly equivalent to a reduction of the Al content in the zeolite, the values of τ_{ind} and $(r_m)_{max}$ on a deactivated zeolite with Si/Al = 44 being intermediate between those for virgin zeolites with Si/Al = 100 and 160.

The acceleration of the rate during the induction period could be due to a change of the properties of the catalyst or due to the changing composition of the gas phase. In one series of experiments at 523 K the reaction was interrupted at a conversion around 20% (that is after the induction period, when the rate of reaction had attained almost its maximum) by shutting off the reactor loop from the mixing turbine. The catalyst was left under a stream of N_2 at reaction temperature while the large volume of the mixing turbine was evacuated and filled anew with pure n-decane in N_2. The course of X vs τ was then reproduced with an induction period and a very low rate at the beginning when the reactor was reconnected; the catalyst itself did not "remember" that it had been in a more active state. If the reactor was disconnected for a period of up to 30 min without changing the composition of the gas in the mixer, then the course of X vs τ resumed at the elevated rate as if no interruption had occurred. A detailed account of

TABLE 2

Induction Period τ_{ind} and Maximum Reaction Rate $(r_m)_{max}$ (Initial Condition p_{A_0} = 2.5 mbar)

Zeolite		T/K	523	573	623	648	673
160/5	(a)	$\frac{\tau_{ind}}{g \cdot s}$ =	1425	1330	580	130	0
100/9	(a)		0	28	16	12	0
44/4	(a)		0	0	<6	10	0
44/4	(b)		420	250			0
160/5	(a)	$\frac{10^6(r_m)_{max}}{mol \cdot g^{-1} s^{-1}}$ =	1.15	0.86	0.14	0.52	0.72
100/9	(a)		33	27	20	8.6	2.5
44/4	(a)		42	50	37	33	13
44/4	(b)		8.6	26	22		12

Note. (a) 1st run on fresh catalyst; (b) 2nd run without preceding regeneration.

these experiments is given in Ref. (*6*). It was concluded from these observations that the acceleration of the reaction depends on the formation of one or more components in the gaseous products, leading to autocatalysis. The modified time τ is therefore the appropriate time-scale to measure the length of the induction period (rather than clock time t), because the rate of change of gas phase composition is proportional to the mass of catalyst in the gradientless closed system.

Several authors (*7–9*) have reported that the rate of cracking of paraffins by solid acid catalysts, especially zeolites, is enhanced by addition of olefins to the feed. We found that the induction period can be fully suppressed if an olefin is added to the starting material *n*-decane. Figure 7 shows X vs τ on zeolite 160/5 (fresh) with and without addition of propene at 523 and 723 K, respectively. With addition of propene the induction period otherwise observed at 523 K vanishes, and the initial rate of reaction is slightly higher than at 723 K, where the addition of propene has no influence on the course of the reaction. A similar result was obtained for zeolite 44/4 where an induction period and autocatalysis was observed at 523 K in the second run if the zeolite was not regenerated, but disappeared when propene was added to reactant *n*-decane in the second run on the partially deactivated zeolite (Fig. 8). In Table 3 the dependence of τ_{ind} and $(r_m)_{max}$ on the partial pressure $(p_{C_3H_6})_0$ of C_3H_6 at $t = 0$ at 523 K for fresh or regenerated zeolite 160/5 is shown. The promoting influence of added C_3H_6 reaches saturation around $p_{C_3H_6} \approx 0.5$ mbar. Without addition of olefins to the reactant the acceleration of the reaction rate ceased at about 50% conversion when the partial pressure of (C_3H_6 + C_4H_8) had reached about 0.4 mbar. Similar results were obtained with addition of *n*-butene or *n*-hexene instead of propene, whereas the addition of *n*-paraffins (C_4–C_6) had no effect on the kinetics.

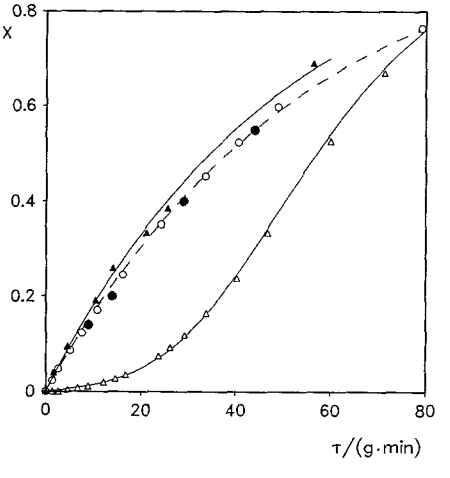

FIG. 7. Influence of addition of propene to reactant *n*-decane on rate of conversion on fresh or regenerated zeolite 160/5; p_{A_0} = 2.5 mbar. T = 523 K: (△) $(p_{C_3H_6})_0 = 0$, (▲) $(p_{C_3H_6})_0$ = 1.5 mbar; T = 723 K: (○) $(p_{C_3H_6})_0 = 0$, (●) $(p_{C_3H_6})_0$ = 1.5 mbar.

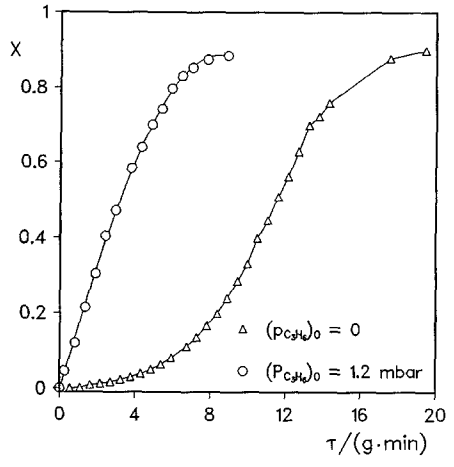

FIG. 8. Influence of addition of propene to reactant *n*-decane on rate of conversion in the second run on partially deactivated zeolite 44/4 at 523 K; p_{A_0} = 2.5 mbar.

(*c*) *Product distribution.* Product distribution was determined as a function of conversion X and of temperature for different Si/Al ratios and crystal sizes of the zeolite. Crystal size and Si/Al ratio were of minor influence on product selectivities. A detailed account of these results can be found in Ref. (*6*). In Table 4 selectivities observed with zeolite 44/4 and p_{A_0} = 2.5 mbar at two temperatures are listed. $(S_i)_0$ are initial selectivities (extrapolated to $X = 0$) whereas $(S_i)_{0.8}$ are integral selectivities obtained at a conversion of *n*-decane of 80%. More than 95% of the carbon initially present in decane was generally found in gaseous products and unconverted decane; products found in only minor amounts are not listed in Table 4.

2. n-Hexane/H-ZSM-5

The reaction of *n*-hexane on zeolite H-ZSM-5 follows a pattern similar to that of *n*-decane in the temperature range 673 to 773 K. It is first order in the concentration of hexane as has been reported already by Olson *et al.* (*11*). With initial partial pressures of n-C_6H_{14} between 2 and 20 mbar, no deactivation of the catalyst was observed. The dependence of the first order rate constant on temperature is shown in Fig. 9 for three zeolites with different Si/Al ratios. k_m for *n*-decane is about 10 times the value found for *n*-hexane on zeolite 100/9 at 723 K. For *n*-hexane an activation energy of 75 kJ/mol is obtained vs 62 kJ/mol for decane, independent of Si/Al-ratio. The data points in Fig. 9 for the most active, relatively Al-rich medium-sized zeolite 22/9 deviate at $T > 730$ K from the Arrhenius line in a way that suggests an influence of intracrystalline mass transfer. On zeolites with Si/Al = 44 the mass-specific rate depends on crystal size for characteristic length $l > 1$ μm at $T = 773$ K, whereas at 723 K it is independent of crystal size up to $l = 2.5$ μm (Fig. 10).

Product distributions observed with zeolite 44/4 at 673 and 773 K and p_{A_0} = 4 mbar are shown in Table 5 as initial selectivities $(S_i)_0$, which are defined as the ratio between the amount of carbon in a given product and the amount of carbon in all products. From these data the initial molar ratio

$$\left(\frac{dn_i}{-dn_{C_6H_{14}}}\right)_{X=0} = \frac{6 \times (S_i)_0}{\varepsilon_i} \qquad (3)$$

can be obtained, where ε_i is the carbon num-

TABLE 3

Influence of Initial Propene Concentration in the Reactant Mixture on the Length of the Induction Period and the Maximum Rate $(r_m)_{max}$

$(p_{C_3H_6})_0$/mbar	0	0.10	0.25	0.46	0.7	1.5
τ_{ind}/(s · g)	1425	648	259	<6	0	0
$(r_m)_{max} \times 10^7$ / mol · s^{-1} · g^{-1}	11	12	13	20	21	21

Note. Catalyst 160/5; initial pressure of decane p_{A_0} = 2.5 mbar; T = 523 K.

TABLE 4

Product Selectivities in the Cracking of *n*-Decane at $X = 0$ and $X = 0.8$.

Product i	$T = 523$ K		$T = 773$ K	
	$(S_i)_0 \times 100$ at $X = 0$	$(S_i)_{0.8} \times 100$ at $X = 0.8$	$(S_i)_0 \times 1000$ at $X = 0$	$(S_i)_{0.8} \times 100$ at $X = 0.8$
C_2H_4	—	0.1	6.3	12.0
C_2H_6	—	—	2.3	2.3
C_3H_6	10.5	7.6	31.7	39.8
C_3H_8	6.2	6.0	4.8	7.0
C_4H_8	16.1	18.0	22.0	17.1
n-C_4H_{10}	10.4	10.3	6.5	6.6
i-C_4H_{10}	10.2	10.1	—	0.5
n-C_5H_{12}	8.3	8.3	6.2	5.6
n-C_6H_{14}	5.0	5.0	5.3	4.3
n-C_7H_{16}	1.9	2.0	3.3	2.1
Benzene + alkylbenzene	—	0.3	—	1.0

Note. Catalyst 44/4; $p_{A_0} = 2.5$ mbar.

ber of product i. It follows from data in Table 5 that 0.75 mol of paraffins are produced per mol of n-hexane reacting at 773 K, whereas at 673 K this ratio is 0.80. The hydrogen balance then requires that molecular hydrogen must also be a product.

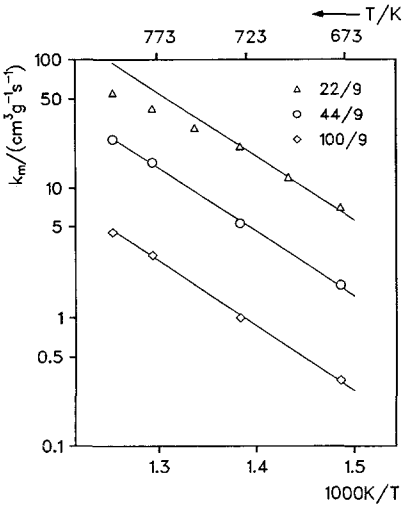

FIG. 9. Dependence of mass-specific first-order rate coefficient k_m for cracking of n-hexane on temperature for zeolites H-ZSM-5 with different Si/Al ratios.

3. n-Decane/HY

Conversion X of n-decane vs τ on dealuminated zeolite Y11 (Si/Al = 11) in the hydrogen form at 673 K is shown in Fig. 11 for two initial partial pressures of reactant. An induction period and autocatalytic behavior was also observed with this zeolite, but only at the low initial partial pressure of 2.5 mbar in the temperature interval between 620 and 720 K. The induction period is prolonged if the zeolite is partially deactivated and it can be suppressed by addition of C_3H_6 to reactant decane. Initial rate of reaction versus temperature exhibits a minimum around 670 K. The pattern of induction period and autocatalysis as well as the unusual temperature-dependence of the reaction rate are thus not phenomena which are peculiar only to zeolite H-ZSM-5; however, they appear to be much less pronounced in the case of HY where they are not easily detected. Carbonaceous deposits are formed in HY at all temperatures up to 773 K, leading to deactivation (*10*). Detailed results concerning kinetics and product distribution for the cracking of decane and hexane in zeolite HY and their dependence on Si/Al-ratio and degree of coking can be found in Ref. (*6*).

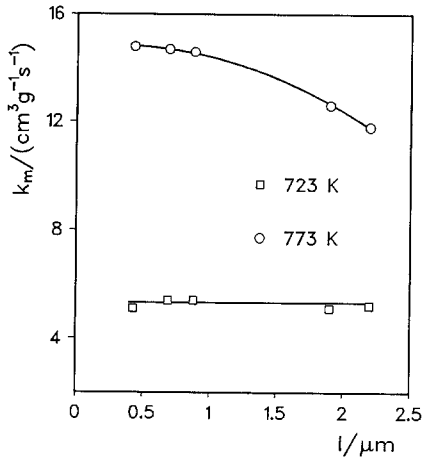

FIG. 10. Dependence of rate coefficient k_m of *n*-hexane cracking on crystal size for H-ZSM-5 with Si/Al = 44.

DISCUSSION

Two phenomena reported above warrant discussion and if possible an explanation: these are the unusual temperature-dependence of the rate of reaction of *n*-decane with concomitant observations of an induction period and autocatalysis and the dependence of cracking rates at elevated temperatures on crystal size.

The "N-shaped" temperature dependence of the initial cracking rate (cf. Fig. 2b) suggests a superposition of two processes in parallel, one of them exhibiting a maximum of rate vs. temperature. Two parallel mechanisms of paraffin cracking on acid catalysts have been postulated by Haag and Dessau (*12*). Route (a) is the classical carbenium ion mechanism of hydride transfer and β-scission (*13, 14*):

$$\left.\begin{aligned} RH + R_1^+ &\rightarrow R^+ + R_1H \\ R^+ &\rightarrow R_1^+ + \text{olefin}, \end{aligned}\right\} \text{(a)}$$

where RH is the original paraffin. R_1^+ is a smaller carbenium ion, resulting from protonation of an olefin which is a prerequisite of the closed sequence. Route (b) is supposedly a monomolecular path of protolytic cracking via a penta-coordinated carbonium ion, requiring a Brønsted acid center; it leads to formation of olefins and molecular hydrogen and can be summarized as

$$\left.\begin{aligned} RH + H^+ &\rightarrow RH_2^+ \\ RH_2^+ &\rightarrow \begin{cases} \text{olefin} + H_2 + H^+ \\ \text{olefin} + \text{paraffin} + H^+. \end{cases} \end{aligned}\right\} \text{(b)}$$

Protolytic and carbenium-ion mechanisms have also been considered by Corma *et al.* (*15*) as simultaneous pathways of paraffin-cracking on Y-zeolites. Haag and Dessau (*12*) concluded from product distribution of hexane-cracking on H-ZSM-5 and HY that pathway (b) prevails at relatively high temperatures, low partial pressures of hydrocarbon and low conversion, the opposite being true for pathway (a), which is favored by elevated olefin concentration in the gas phase. This result was confirmed and extended to other zeolite structures with varying Si/Al ratio by Wielers *et al.* (*16*).

We found that the initial molar ratio of paraffin produced to *n*-hexane converted on ZSM-5 at $T \geq 673$ K is substantially smaller than one, which shows that there is a contribution from the protolytic route producing molecular hydrogen. We now compare the pattern of the kinetics of paraffin-cracking to be expected for the dual mechanism pro-

TABLE 5

Initial Selectivities $(Si)_0 \times 100$ in the Cracking of *n*-Hexane on Zeolite 44/4

Product *i*	CH_4	C_2H_4	C_2H_6	C_3H_6	C_3H_8	C_4H_8	C_4H_{10}	C_5H_{10}	$\Sigma S_i \times 100$
T = 673 K	1	4	12	39	15	25	5	1	102
T = 773 K	1.5	7	11.6	41	13	22.6	3.3	0.6	100

Note. $(p_{C_6H_{14}})_0$ = 4.0 mbar.

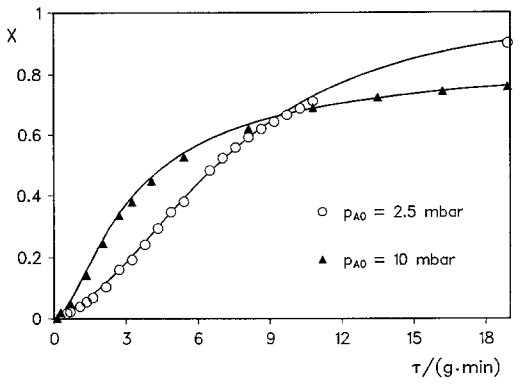

FIG. 11. Conversion X of n-decane vs τ on zeolite HY with Si/Al = 11 at 673 K for two initial pressures of reactant.

posed by Haag and Dessau (*12*) with the experimental observations reported here. Assuming as rate limiting hydride transfer in sequence (a), formation of RH_2^+ in sequence (b), one obtains from simple mass action the rate equations

$$r_a = k_{a1} \cdot [H^+]_o \cdot \Theta_{Ol} \cdot [A] \qquad (4a)$$

$$r_b = k_{b1} \cdot [H^+]_o \cdot (1 - \Theta_{Ol}) \cdot [A], \qquad (4b)$$

where $[H^+]_o$, [A] are the intracrystalline concentration of Brønsted centers or educt paraffin A, respectively, and Θ_{Ol} is the fraction of Brønsted centers occupied by carbenium ions R^+. The observable mass specific reaction-rate r_m of educt A is then

$$-\frac{1}{m} \cdot \frac{dn_A}{dt} \equiv r_m = r_a + r_b$$

$$r_m = [k_a \cdot \Theta_{Ol} + k_b \cdot (1 - \Theta_{Ol})] \cdot c_A, \qquad (5)$$

where c_A is the concentration of A in the gas phase, proportionality $[A] \sim c_A$ being assumed. k_a and k_b are mass-specific first-order rate constants depending on zeolite composition ($[H^+]_o$) and temperature; their units are $[k_{a,b}] = cm^3\ g^{-1}\ s^{-1}$. A relation of the approximate form

$$\Theta_{Ol}^* = \frac{K \cdot c_{Ol}}{1 + K \cdot c_{Ol}} \qquad (6)$$

can be expected to describe the equilibrium (*) between Brønsted centers occupied by carbenium-ions and olefins in the gas phase, wherein K decreases with increasing temperature. If product-olefins are desorbing we must have $\Theta_{Ol} > \Theta_{Ol}^*$. Figure 12 depicts schematically that the antagonistic temperature dependence of k_a and k_b on the one hand and of K on the other hand can result in an N-shaped form of r_m vs T, where a minimum in r_m follows after a maximum.

For the left-hand side of Eq. (5) we have for our closed system

$$r_m = V \cdot c_{A_0} \cdot \frac{dX}{d\tau} \qquad \text{where } V = 7100\ cm^3.$$

With

$$c_A = c_{A_0} \cdot (1 - X),$$

Eq. (5) can be rewritten in observable variables X and τ,

$$\frac{dX}{d\tau} = \frac{1}{V}[k_a \cdot \Theta_{Ol} + k_b(1 - \Theta_{Ol})] \cdot (1 - X), \qquad (7)$$

wherein Θ_{Ol} can depend on X, T, and initial conditions. The limiting case $\Theta_{Ol} = 0$, leading to the first-order law

$$\ln \frac{1}{1 - X} = \frac{k_b}{V} \cdot \tau \qquad (8)$$

has to be expected at sufficiently elevated temperatures. We therefore tentatively identify the first-order rate coefficient k_m obtained in the high-temperature regime of decane- and hexane-cracking on ZSM-5 as the rate coefficient k_b of protolytic cracking.

We will have $0 < \Theta_{Ol} < 1$ when we go to lower temperatures, where both terms in the square brackets of Eq. (7) have to be considered. In the temperature interval between the extrema of the initial rate we may approximate Θ_{Ol} as $\Theta_{Ol} \approx K \cdot c_{Ol}$ (cf. Fig. 12) and let $c_{Ol} = \nu_{Ol} \cdot c_{A_0} \cdot X$, where ν_{Ol} is a dimensionless stoichiometric number. We have then from Eq. (7)

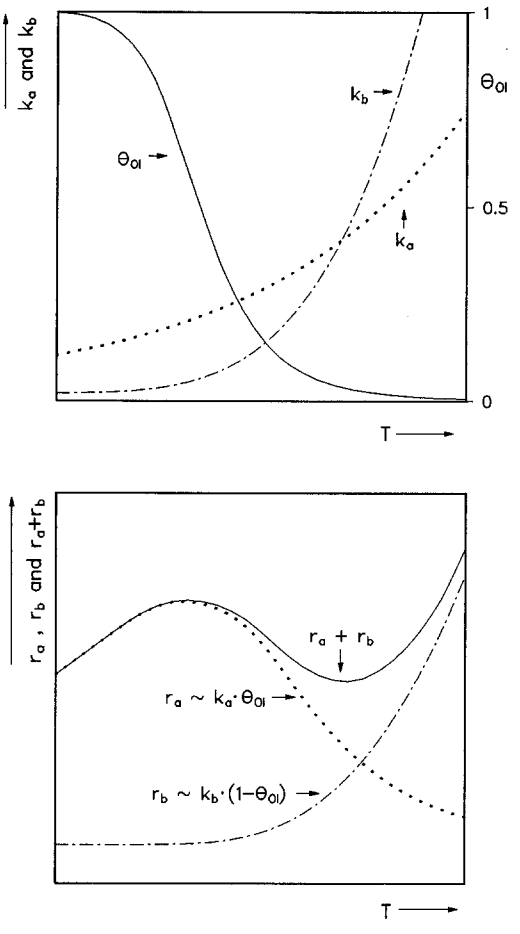

FIG. 12. Temperature-dependence of k_a, k_b, and Θ_{Ol} leading to "N-shaped" form of r_m vs T for given gas-phase concentrations c_A and c_{Ol} (schematic).

$$\frac{dX}{d\tau} = \frac{1}{V}[k_b + (k_a - k_b) \cdot \nu_{Ol} \cdot K \cdot c_{A_0} \cdot X](1 - X), \quad (9)$$

which has the form

$$\frac{dX}{d\tau} = \alpha \cdot X \cdot (1 - X) + \beta \cdot (1 - X) \quad (10)$$

with

$$\alpha \equiv \frac{(k_a - k_b) \cdot K' \cdot c_{A_0}}{V}; \quad K' \equiv K \cdot \nu_{Ol}. \quad (11a)$$

$$\beta \equiv \frac{k_b}{V} \quad (11b)$$

The first term on the right-hand side of Eq. (10) is initially zero and increases with conversion (autocatalysis); it reaches a maximum at $X = 0.5$. Integration of Eq. (10) with initial condition $X = 0$ at $\tau = 0$ yields

$$\ln \frac{X + \beta/\alpha}{1 - X} = (\alpha + \beta) \cdot \tau + \ln(\beta/\alpha). \quad (12)$$

According to Eq. (12) an induction period

$$\tau_{ind} = \frac{(\alpha/\beta + 1) \cdot \ln(\alpha/\beta) - 2 \cdot (\alpha/\beta + 1)}{(\alpha/\beta + 1)(\alpha + \beta)} \quad (13)$$

has to be expected if $\alpha > \beta$ holds.

The ratio of the rates of cracking via routes (a) and (b) depends on α/β and on conversion X. Equation (12) simplifies to

$$\ln \frac{X}{1 - X} \approx \alpha \cdot \tau + \ln(\beta/\alpha) \quad (14)$$

for $\beta/\alpha < 10^{-2}$ and $X > 0.01$. The observable patterns $\ln X/(1 - X)$ vs τ and X vs τ according to Eqs. (12) and (14) are shown schematically in Fig. 13. They correspond to experimental observations reported above for cracking of *n*-decane on H-ZSM-5 at temperatures below 650 K and on HY between 620 and 720 K. The formalism (model) of Eqs. (4) to (14) must be viewed as an approximation based on simplifying assumptions. Nevertheless it not only explains the peculiar temperature-dependence of the reaction rate but also a few other experimental observations.

An induction period and autocatalysis were observed on H-ZSM-5 and HY only at temperatures below certain upper limits. According to the model, an induction period and autocatalysis should be observed only if the inequality $\alpha/\beta > 1$ holds. The inequality $\alpha/\beta > 1$ is tantamount to

$$\frac{k_a \cdot K' \cdot c_{A_0}}{1 + K' \cdot c_{A_0}} > k_b$$

as follows from Eq. (11). The equilibrium constant K for the exothermic chemisorption of olefins must decrease strongly with T; the phenomena of an induction period and autocatalysis can therefore be expected

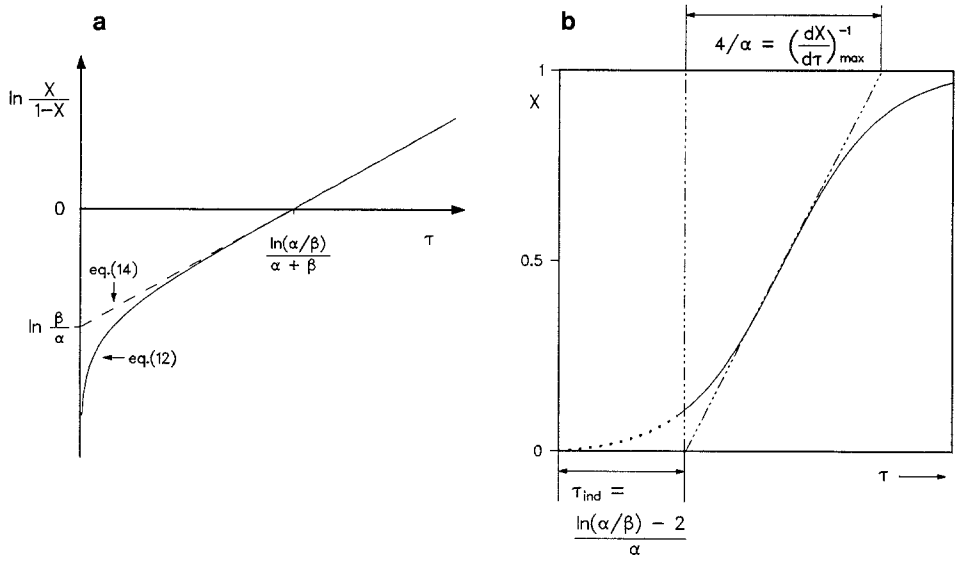

FIG. 13. (a) ln $X/(1 - X)$ vs τ according to Eqs. (12) and (14); (b) X vs τ according to Eq. (14).

to disappear at sufficiently elevated temperatures. The length of an induction period was found to increase with the Si/Al ratio and through deactivation of the zeolite. According to the model, τ_{ind} should be proportional to $(\alpha + \beta)^{-1}$ at constant α/β, which means inversely proportional to the activity of the zeolite. Very short induction periods cannot be observed and their length then appears to be zero.

The induction period and autocatalysis can be suppressed completely when light olefins are added to the reactant *n*-decane, the initial rate of reaction then being slightly higher than the maximum rate after an induction period. The model predicts that saturation of acid sites by carbenium ions is reached ($\Theta_{Ol} = 1$) with increasing olefin concentration in the gas phase, so that Eq. (5) simplifies to

$$r_m = k_a \cdot c_A \qquad (15)$$

and the first-order rate equation

$$\frac{dX}{d\tau} = \frac{k_a}{V}(1 - X) \qquad (16)$$

results for $K \cdot c_{Ol} \gg 1$, $\Theta_{Ol} = 1$.

Whereas the model predicts that autocatalysis and induction period vanish at elevated temperatures, as was always observed, it does not explain that these phenomena can also vanish when the temperature is lowered, as observed for H-ZSM-5 with Si/Al $\leq$ 100 (cf. Table 2). The rate of desorption of chemisorbed olefin will decrease strongly when the temperature is lowered and the equilibrium assumption $\Theta_{Ol} = \Theta^*_{Ol}$ which Eq. (9) implies is then perhaps no longer applicable.

A quantitative evaluation of the experimental results has to take into account that zeolite ZSM-5 initially deactivates to a limited extent at $T < 650$ K, whereas the kinetic formalism assumes k_a and k_b (and consequently also α and β) to be constant in time. Zeolite 44/4 lost about 70% of its initial activity within 60 min at 523 K in a stream of *n*-decane (2.5 mbar) and nitrogen, whereafter its activity remained constant. The kinetics of *n*-decane cracking were then observed in the closed system on this partially deactivated zeolite with now constant properties; the result is shown in Fig. 14. From the ordinate-intersection and the slope of ln $X/$

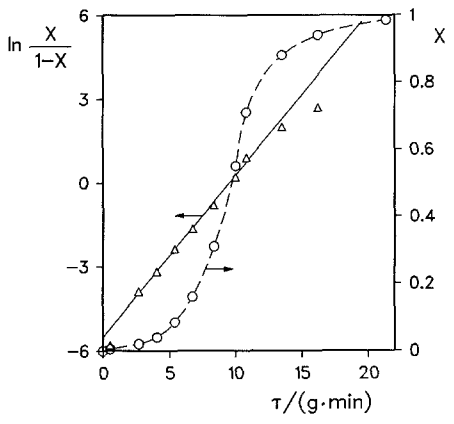

FIG. 14. Conversion of *n*-decane on zeolite 44/4 with constant activity after partial deactivation at 523 K; p_{A_0} = 2.5 mbar. Left ordinate: $\ln(X/(1-X))$ vs τ (Eq. (14)); right ordinate: X vs τ.

$(1 - X)$ vs τ we obtain $\alpha = 0.58\ g^{-1}\ min^{-1}$, $\beta = 2.4 \times 10^{-3}\ g^{-1}\ min^{-1}$ and through Eq. (11b) the rate coefficient of protolytic cracking at 523 K as $k_b = 0.28\ cm^3\ g^{-1}\ s^{-1}$. The rate coefficient k_a for the carbenium-ion mechanism cannot be obtained from these data because the coefficient α according to Eq. (11a) contains the product $k_a \cdot K'$. However, k_a can be obtained from the kinetics with added propene, which was observed for the same catalyst at 523 K, p_{A_0} = 2.5 mbar, $(p_{C_3H_6})_0$ = 1.1 mbar and found to follow exactly Eq. (16) with $k_a = 29\ cm^3\ g^{-1}\ s^{-1}$. For partially deactivated zeolite ZSM-5 with Si/Al = 44 we then have $k_a/k_b \approx 100$ for the ratio of rate coefficients at 523 K.

The decline of activity of zeolites ZSM-5 and HY with time-on-stream (t_{OS}) during the cracking of paraffins can be described by

$$\left.\begin{aligned} r_m &= f\{\text{compos.}, T\} \cdot \Omega\{t_{OS}\} \\ \text{with } \Omega\{t_{OS}\} &= \Omega_\infty + (1 - \Omega_\infty) \\ &\quad \cdot \exp\{-k_d \cdot t_{OS}\} \end{aligned}\right\} \quad (17)$$

as has been shown previously (*10*). Ω is the fraction of initial activity remaining at t_{OS}; Eq. (17) stipulates that kinetics of reaction and deactivation are "separable."

Experimental results for virgin or regenerated zeolite ZSM-5 at $T < 650$ K were fitted to the rate equation

$$\frac{dX}{d\tau} = \frac{\Omega\{t_{OS}\}}{V}[k_b + (k_a - k_b) \cdot K' \cdot c_{A_0}](1 - X), \quad (18)$$

where t_{OS} equals clock time t from the start of the run. Figure 15 shows observed points $X\{\tau\}$ for *n*-decane cracking on virgin zeolite 160/5 at 523 K and X vs τ computed according to Eqs. (17) and (18) with fitted parameters $(k_a - k_b) \cdot K' \cdot c_{A_0} = 56\ cm^3\ g^{-1}\ s^{-1}$, $k_b = 0.17\ cm^3\ g^{-1}\ s^{-1}$; $k_d = 1.7 \times 10^{-4}\ s^{-1}$, and $\Omega_\infty = 0.5$. The dotted line was computed with the same rate coefficients for $\Omega_\infty = 1$, that is, without taking deactivation into account. The rate constant k_b of protolytic cracking can be obtained independently for the fresh catalyst 160/5 by extrapolating the first-order rate coefficient k_m observed with this catalyst at elevated temperatures (cf. Fig. 5), since it was concluded that the rate at $T > 700$ K and p_{A_0} = 2.5 mbar is essentially due to the protolytic pathway. This extrapolation yields k_m (523 K) = $0.12\ cm^3\ g^{-1}\ s^{-1}$, in fair agreement with the value of $0.17\ cm^3\ g^{-1}\ s^{-1}$ obtained by multiparameter-fitting in Eq. (18). The pattern of the kinetics thus agrees in a rather wide range of temperature with expectation

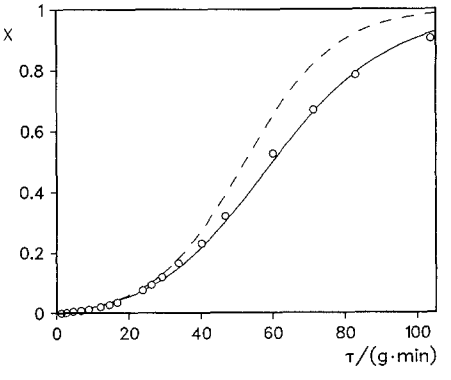

FIG. 15. Conversion X of *n*-decane on fresh zeolite 160/5 versus τ at 523 K; p_{A_0} = 2.5 mbar. Experimental observation (○) and reproduction through Eq. (18), taking into account deactivation (—) or assuming constant activity (– – –). For parameters, see text.

assuming the dual mechanism postulated by Haag and Dessau (*12*).

An influence of crystal size on cracking rates was observed only for rather large crystals ($l > 1$ μm) of ZSM-5 with Si/Al < 50 in the temperature range above 720 K. Intracrystalline mass transfer resistance therefore needed not to be considered as a possible complication in the above discussion of the kinetics at temperatures below 650 K. The observed influence of crystal size on cracking rates of hexane and decane at elevated temperatures (cf. Figs. 5 and 10) can be understood as resulting from superposition of first-order reaction and diffusion of reactant paraffin in the crystal, following classical theory (*17, 18*). From the ratios of the rates observed on small and large crystals, respectively, we obtain the following intracrystalline effectiveness factors η and Thiele numbers φ in zeolite H-ZSM-5, Si/Al = 44, crystal size 36 × 10 × 10 μm^3 (l = 2.2 μm):

for n-hexane at 773 K:	η = 0.80;	
	φ = 0.86	
for n-decane at 723 K:	η = 0.66;	
	φ = 1.32	

From these data the intracrystalline diffusivity D_{intra} under reaction conditions can be estimated as

$$D_{\text{intra}} = \frac{L^2 \cdot k_m \cdot \rho_z}{\eta \cdot \varphi^2} \cdot c_A/\tilde{c}_A, \qquad (19)$$

where L = 5 μm is half the thickness of the plate-shaped crystals, ρ_z = 1.8 g cm^{-3} is their density, and $c_A/\tilde{c}_A$ is the ratio of gas-phase concentration c_A of reactant A and its volumetric concentration $\tilde{c}_A$ in the zeolite crystal (*19*). For *n*-hexane in H-ZSM-5 one obtains $D_{\text{intra}} \approx 2.5 \times 10^{-10}$ m^2 s^{-1} at 773 K with $c_A/\tilde{c}_A = 0.25$, in reasonable agreement with Voogd and van Bekkum (*20*). For *n*-decane at 723 K we have $D_{\text{intra}} = 10^{-10}$ m^2 s^{-1}, assuming $c_A/\tilde{c}_A = 0.03$. These values of D_{intra} appear to be rather low compared to diffusivities characterizing the rate of sorption into ZSM-5 at the much lower temperature of 300 K, diffusion in zeolites being an activated process. The rate of sorption of *n*-hexane into H-ZSM-5 (Si/Al = 35) corresponds to $D > 7 \times 10^{-10}$ m^2 s^{-1} at 298 K (*21*). The discrepancy is probably due to the presence under reaction conditions of less mobile products and intermediates (such as carbenium ions) which are absent when rates of sorption of pure paraffins are observed. It has been shown that small amounts of olefins or benzene in zeolite ZSM-5 retard rates of sorption and self-diffusion of paraffins considerably (*22, 23*). It follows that diffusivities obtained from sorption kinetics or self-diffusion of pure compounds in zeolites at room temperature are of limited significance with respect to the rate of catalytic reactions at more elevated temperature.

APPENDIX: NOTATION

c_{A_0}, c_A	concentration of reactant A in the gas phase at t = 0 and at t, respectively	mol/cm^3
$\tilde{c}_A$	volumetric concentration in zeolite crystal	mol/cm^3
c_{Ol}	concentration of olefins in the gas phase	mol/cm^3
K	equilibrium constant for chemisorption of olefins at Brønsted centers, eq. (6)	cm^3/mol
k_a	rate coefficient for autocatalytic cracking	cm^3/(g · s)
k_b	rate coefficient for protolytic cracking	cm^3/(g · s)
k_m	observed mass-specific first-order rate coefficient	cm^3/(g · s)
l	characteristic length of crystal (volume/surface)	μm
m	mass of zeolite catalyst in the reactor	g
p_{A_0}	initial pressure of	mbar

	reactant A	
r_m	reaction rate of reactant A per unit mass of catalyst	mol/(g · s)
S_i	selectivity of conversion of reactant A to hydrocarbon i, Eq. (2)	—
t	clock time from start of reaction	s
t_{OS}	time on stream of catalyst	s
T	temperature of catalyst	K
V	volume of closed system	cm^3
X	conversion of reactant A	—
y	carbon fraction	—
α, β	phenomenological rate coefficients, Eq. (10)	$g^{-1}\ s^{-1}$
ε_i	carbon number of compound i	—
η	intracrystalline effectiveness factor	—
Θ_{Ol}	fraction of Brønsted centers occupied by carbenium ions	—
ρ	density of crystal	g/cm^3
τ	modified time $t \cdot m$	g · s
τ_{ind}	induction period (Fig. 6)	g · s
φ	intracrystalline Thiele number, characterizing zeolite crystal	—
Φ	intercrystalline Thiele number, characterizing pellet	—
Ω	fraction of initial activity remaining at t_{OS}	—

ACKNOWLEDGMENTS

We are indebted to G. T. Kokotailo for his help and advice in the synthesis and characterization of zeolites and to K. Beschmann for helpful and stimulating discussions. This work was supported by the Deutsche Forschungsgemeinschaft as a project in Sonderforschungsbereich 250.

REFERENCES

1. Jacobs, P. A., "Carboniogenic Activity of Zeolites." Elsevier, Amsterdam, 1977.
2. Venuto, P. B., and Habib, Jr., E. T., "Fluid Catalytic Cracking with Zeolite Catalysts." Dekker, New York, 1979.
3. Wojciechowski, B. W., and Corma, A., "Catalytic Cracking." Dekker, New York, 1986.
4. (a) Beyer, H. K., Belenykaja, I. M., and Hange, F., *J. Chem. Soc. Faraday Trans. 1* **81,** 2889 (1985); (b) Breck, D. W., and Flanigan, E. M., in "Molecular Sieves", p. 47, Society of Chemical Industry, London 1968.
5. Prinz, D., and Riekert, L., *Appl. Catal.* **37,** 139 (1988).
6. Zhou, J.-Q., "Kinetik der katalytischen Spaltung von n-Hexan und n-Dekan an Zeolithen HY und H-ZSM-5." Dissertation, Karlsruhe, 1991.
7. Pansing, W. F., *J. Phys. Chem.* **69,** 392 (1966).
8. Weisz, P. B., *Annu. Rev. Phys. Chem.* **21,** 189 (1970).
9. Anufriev, D. M., Kuznetsov, P. N., and Ione, K. G., *J. Catal.* **65,** 221 (1980).
10. Hammon, U., Kokotailo, G. T., Riekert, L., and Zhou, J.-Q., *Zeolites* **8,** 338 (1988).
11. Olson, D. H., Haag, W. O., and Lago, R. M., *J. Catal.* **61,** 390 (1980).
12. Haag, W. O., and Dessau, R. M., *in* "Proceedings, 8th International Congress on Catalysis, Berlin, 1984," Vol. II, p. 305, Verlag Chemie, Weinheim, 1984.
13. Greensfelder, B. S., Voge, H. H., and Good, G. M., *Ind. Eng. Chem.* **41,** 2573 (1949).
14. Thomas, C. T., *Ind. Eng. Chem.* **41,** 2564 (1949).
15. Corma, A., Planelles, J., and Tomas, F., *J. Catal.* **94,** 445 (1985).
16. Wielers, A. F. H., Vaarkamp, M., and Post, M. F. M., *J. Catal.* **127,** 51 (1991).
17. Damköhler, G., "Der Chemie-Ingenieur," Vol. III, 1, p. 430, Leipzig, 1937.
18. Thiele, E. W., *Ind. Eng. Chem.* **31,** 916 (1939).
19. Heering, J., Kotter, M., and Riekert, L., *Chem. Eng. Sci.* **37,** 581 (1982).
20. Voogd, P., and van Bekkum, H., *Appl. Catal.* **59,** 311 (1990).
21. Beschmann, K., Fuchs, S., and Riekert, L., *Zeolites* **10,** 798 (1990).
22. Prinz, D., and Riekert, L., *Ber. Bunsenges. Phys. Chem.* **90,** 413 (1986).
23. Förste, C., Germanus, A., Kärger, J., Pfeifer, H., Caro, J., Pilz, W., Zikánová, A., *J. Chem. Soc. Faraday Trans. 1* **83,** 2301 (1987).